HHS Public Access

Author manuscript

J Expo Sci Environ Epidemiol. Author manuscript; available in PMC 2023 January 04.

Published in final edited form as:

J Expo Sci Environ Epidemiol. 2017 March ; 27(2): 184–192. doi:10.1038/jes.2016.9.

Use of mobile and passive badge air monitoring data for NO_x and ozone air pollution spatial exposure prediction models

Wei Xu[1,2], **Erin A. Riley**[2], **Elena Austin**[2], **Miyoko Sasakura**[2], **Lanae Schaal**[3], **Timothy R. Gould**[4], **Kris Hartin**[2], **Christopher D. Simpson**[2], **Paul D. Sampson**[3], **Michael G. Yost**[2], **Timothy V. Larson**[2,4], **Guangli Xiu**[1], **Sverre Vedal**[2]

[1]Department of Environmental Engineering, East China University of Science and Technology, Shanghai, China

[2]Department of Environmental and Occupational Health Sciences, University of Washington, Seattle, Washington, USA

[3]Department of Statistics, University of Washington, Seattle, Washington, USA

[4]Department of Civil and Environmental Engineering, University of Washington, Seattle, Washington, USA.

Abstract

Air pollution exposure prediction models can make use of many types of air monitoring data. Fixed location passive samples typically measure concentrations averaged over several days to weeks. Mobile monitoring data can generate near continuous concentration measurements. It is not known whether mobile monitoring data are suitable for generating well-performing exposure prediction models or how they compare with other types of monitoring data in generating exposure models. Measurements from fixed site passive samplers and mobile monitoring platform were made over a 2-week period in Baltimore in the summer and winter months in 2012. Performance of exposure prediction models for long-term nitrogen oxides (NO_X) and ozone (O_3) concentrations were compared using a state-of-the-art approach for model development based on land use regression (LUR) and geostatistical smoothing. Model performance was evaluated using leave-one-out cross-validation (LOOCV). Models performed well using the mobile peak traffic monitoring data for both NO_X and O_3, with LOOCV R^2s of 0.70 and 0.71, respectively, in the summer, and 0.90 and 0.58, respectively, in the winter. Models using 2-week passive samples for NO_X had LOOCV R^2s of 0.60 and 0.65 in the summer and winter months, respectively. The passive badge sampling data were not adequate for developing models for O_3. Mobile air monitoring data can be used to successfully build well-performing LUR exposure prediction models for NO_X and O_3 and are a better source of data for these models than 2-week passive badge data.

Correspondence: Professor Guangli Xiu, Department of Environmental Engineering, East China University of Science and Technology, Shanghai, China., Tel.: +86 021 64241927. Fax: +86 021 64241927., xiugl@ecust.edu.

CONFLICT OF INTEREST

The authors declare no conflict of interest.

Supplementary Information accompanies the paper on the Journal of Exposure Science and Environmental Epidemiology website (http://www.nature.com/jes)

Keywords

air pollution monitoring; exposure models; land use regression; partial least squares; universal kriging

INTRODUCTION

Exposure prediction is an essential part of any air pollution epidemiology study. Since exposure to outdoor air pollution is never directly measured, there is heavy reliance on exposure modeling. Various types of exposure models have been used for estimating air pollution exposure. These can be classified into: (1) geostatistical models that use methods such as proximity to monitors, interpolation, and land use regression (LUR); (2) dispersion models (e.g., Gaussian models) and integrated meteorological emission models; and (3) hybrid or fusion models that combine monitoring data with a dispersion or integrated meteorological emission model.[1,2] The geostatistical models (and fusion models) make use of air pollution monitoring data generated from some type of air monitoring network, whereas monitoring data are typically not used by dispersion-type models.

Most often, routinely collected administrative air monitoring data, such as those collected in the US Environmental Protection Agency's (EPA) Air Quality System (AQS), are used when air pollution monitoring data are needed for building geostatistical models.[3–5] However, because of limitations in routinely collected data due to interrupted sampling schedules and sparse spatial coverage, purpose-designed monitoring is sometimes carried out to improve temporal or spatial coverage, or both. Better spatial coverage has the added benefit of allowing estimates of exposure at small spatial scales that is often desired in attempting to reduce exposure measurement error. Passive samplers (badges) for some gaseous pollutants have been used in monitoring campaigns designed to estimate exposure in the context of specific health studies, with 1- or 2-week samples typically collected several times over the duration of a study; these have been shown to produce data that are highly correlated with continuous monitoring data.[1] Models for oxides of nitrogen (NOx), for example, have been successfully built using passive sampler monitoring data and LUR modeling approaches.[6–11] Mobile monitoring, in which a vehicle equipped with real-time air monitoring equipment is driven on prescribed routes, has generally been used in small regional monitoring campaigns or to identify regional or traffic-related pollution sources. Padro-Martinez et al. used mobile monitoring to observe decreasing trends in PM, NO and NO_2 concentrations with increasing distances from main roads.[12] Norris and Larson used mobile monitoring in the Seattle region to generate data to inform NO_2 monitor siting.[13] Mobile monitoring data are less commonly used for building exposure models. Larson et al. used mobile monitoring in Vancouver, Canada, together with LUR to generate surfaces of black carbon and light absorption coefficient.[14,15] Montagne et al. used mobile monitoring in the Netherlands to build LUR models for ultrafine particles and black carbon.[16] Mobile monitoring has the advantage of efficiently sampling a large number of locations in an urban area, albeit for only limited periods of time at each location, and may be especially useful for monitoring of pollutants that exhibit substantial diurnal variation[17,18] or that cannot be measured using passive samplers.

Here we report findings from a study that employed passive and mobile air monitoring campaigns in parallel in Baltimore, MD, in the summer and winter seasons. This allowed us to build and to compare the performance of sophisticated long-term exposure prediction models for NO_X and ozone (O_3) that were generated concurrently from either passive badge data or mobile monitoring data using LUR and geostatistical smoothing (kriging) methods.

METHODS

Monitoring Data and Preprocessing

We selected 43 sampling sites in Baltimore, MD (Figure 1), to provide reasonably regular spatial coverage of the area of participant locations of the Multi-Ethnic Study of Atherosclerosis cohort in Baltimore. The monitoring campaigns took place in the winter (11–22 February) and the summer (18–27 June) months of 2012. Two types of monitoring methods were utilized. One was a passive sampling method using fixed Ogawa badge passive samplers to obtain a cumulative sample over the 10- to 12-day sampling period at each of the 43 sites (NO, NO_2, NO_X, and O_3 Sampling Protocol Using the Ogawa Sampler; Ogawa and Company, USA, Inc.: Pompano Beach, FL, USA, 1998). Duplicate passive samples were obtained at eight randomly chosen sites of the 43 sampling sites for assessing measurement precision; duplicate concentrations were averaged for these sites.

The other method employed a mobile monitoring platform described elsewhere,[19] in which monitors were housed in a vehicle that was driven during peak traffic hours (1400 to 1900 hours) over a prescribed route that passed several times through each of the 43 sites. A large three-loop route anchored at a fixed monitoring site (site #1 in Figure 1), with 15 sites per loop (14 unique sites and the fixed site), was driven repeatedly with each loop driven once during each 3- to 4-day period of the 10- to 12-day campaign concurrent with the passive monitor sampling in both the summer and winter seasons (see details in online Supplementary Table 1). In addition, each of the 43 sites (termed “fuzzy points”) was centered within a 300-m radius of a small four-leaf cloverleaf route that was driven once on each of 3 days and took 5–8 min to complete (Figure 1 inset). Ten-second continuous concentrations and corresponding global positioning system coordinates were obtained at all times along the routes. Ten-second measurements were also made at the fixed site (site #1) where a passive monitor also obtained cumulative measurements concurrently. O_3 and NO_X were measured by an Ozone Analyzer 3.02P-A and a NO Model 410, Converter 410, respectively, in both the mobile and fixed monitoring platforms.[19] Hourly NO_X and O_3 concentration data were also obtained from two AQS monitoring sites (one for NOx and one for O_3, Figure 1). Fixed site and AQS monitoring data were used for adjusting measurements for temporal variation in concentrations (see below).

Because each route was driven at different times on different days, the mobile monitoring data required adjustment using fixed site or AQS monitoring data. Time adjustment adjusted each 10-s measurement for the hourly or afternoon (1400 to 1900 hours) variation in pollutant concentrations relative to the 2-week average concentration. In the winter, concentrations were adjusted by hourly averaged values of the one fixed monitoring site. Because the NO_X and O_3 data in the summer at the fixed site had many missing values, and there was good agreement of the fixed site with the AQS site (R^2 = 0.75 for NOx and R^2

= 0.83 for O_3), the mobile NO_X and O_3 concentrations in the summer were adjusted using corresponding afternoon averaged concentrations (1400 to 1900 hours) of the AQS sites. Equation (1) shows the time adjustment arithmetic:[12]

$$\mathrm{Conc_{adj}} = \mathrm{Conc_{orig}} \times (\mathrm{Conc_{2wk}}/\mathrm{Conc_{hr}}) \quad (1)$$

where $\mathrm{Conc_{adj}}$ is the final adjusted 10-s concentration; $\mathrm{Conc_{orig}}$ is the raw 10-s mobile monitoring concentration; $\mathrm{Conc_{hr}}$ is the corresponding hourly or afternoon averaged fixed or AQS site concentration; and $\mathrm{Conc_{2wk}}$ is the average concentration for the afternoon periods over the 10 or 12 days (~2 weeks) at the fixed or AQS site. When the hourly or afternoon concentration was the same as the 2-week average, there was no adjustment. When the hourly or afternoon concentration was lower than the 2-week average, the original 10-s concentration was adjusted upwards, and when the hourly or afternoon concentration was higher than the 2-week average, the original concentration was adjusted downwards. To remove extreme and negative values, each data set was initially trimmed at four times the interquartile range. After time adjustment, the median NO_X concentration (to avoid the influence of extreme outliers) and mean O_3 concentration at each site were used as the raw data for the models.

Geographic Data

More than 300 geographic variables were available from our database to be used as potential LUR covariates, of which 257 were retained after excluding uninformative variables that showed limited variation (Table 1). Categories of variables included: (1) population (US Census Bureau, 2001); (2) distance to and length of major roads (for A1, A2, and A3 census feature class codes) and their mutual intersections (TeleAtlas Dynamap, 2000); (3) distance to relevant sites (commercial, city hall, airport, shipping port, railways, and railway yards[20]) (4) percentage of 12 kinds of land use categories (see Table 1[21]) (5) summaries of Normalized Difference Vegetation Index (NDVI),[22] a measure of green space; (6) percentage of impervious surfaces; (7) elevation[23] and (8) total emissions of CO, NOX, $PM_{2.5}$, PM_{10}, SO_2 (in tons per year[24]). Except for the distance to features variables, all variables were specified as feature within circular buffers of increasing radii. Table 1 shows details of the geographic variables and the buffer sizes used.

In order to produce maps that reflect the spatial heterogeneity of our exposure models, geographic covariates were calculated for grid points at several different resolutions. Grids were designed to show the outlying areas of Baltimore at a 1 – 1 km resolution and the center of city area at a 500 × 500 m^2 resolution.

Prediction Models

Conceptually, the prediction models are generated in a two-step process in which residuals from a LUR that are spatially correlated are smoothed (interpolated) using kriging. In practice, the regression and smoothing steps are combined in universal kriging (UK) as in Sampson et al.[25] The large number of geographic variables were first reduced using partial least squares (PLS) regression. PLS is conceptually similar to principal components analysis, with the PLS components, in contrast to principal components analysis

components, being computed as linear combinations of the original covariates to maximize the covariance between the dependent variable and the independent components. Details are presented in Sampson et al.[25] PLS regressions were performed using the PLS package[26] in R (R Core Team). The kriging parameters (nugget τ^2, partial sill σ^2 and range φ^2) and the final regression coefficients of the UK model were estimated by maximum likelihood using the GeoR package in R.

In all, there are eight sets of pollutant data: two monitoring methods for each of two seasons for both O_3 and NO_X. For PLS, O_3 and NO_X were centered and geographic variables were centered and standardized by their variance. For UK, in addition, badge NOx data and mobile O_3 data were square root transformed and mobile NO_X data were standardized by their variance. Geographic covariates at unobserved locations (i.e., residences of cohort members) were then used to predict concentrations at those locations using the prediction models.

Evaluation of Model Performance

Leave-one-out cross-validation (LOOCV) was used for evaluation of model performance and to determine the number of PLS components. Each monitoring site was excluded and models were rerun using data from the other remaining 42 sites. Predicted and monitored values were then used to calculate errors. Model performance statistics included cross-validated root mean squared prediction error (RMSEP) and the cross-validated R^2, calculated as 1-RMSEP^2/Var(Obs) on transformed data scales.

RESULTS

Monitoring Results

NO_X and O_3 concentrations monitored at the 43 sites using the two approaches both in the summer and the winter are shown in Figure 2. High concentrations of NO_X were more typically present in the center of the city (sites 1–4, 15–16, 29–31): maximum of 37 and 74 p.p.b. for badge samples in the summer and the winter, respectively, and 23 and 38 p.p.b. for mobile samples in the summer and the winter, respectively. Lower concentrations were observed in less central areas (sites 7–9, 24–26, 38–40) with minimums of 5.5 and 23 p.p.b. for badge samples in the summer and the winter, respectively, and −2.1 and 2.4 p.p.b. for mobile samples in the summer and the winter, respectively. The pattern of mobile O_3 concentrations across sites was nearly the mirror image of that of NO_X. The mobile O_3 concentrations, and both badge and mobile NO_X concentrations, had similar spatial trends in the two seasons. For the badge O_3 data, there was little spatial variability in the summer. For NO_X, both monitoring approaches measured generally higher levels in the winter, and higher O_3 concentrations in the summer, although there were more exceptions to this for O_3 badge data.

Building the Models

Table 2 presents summaries of the leave-one-out cross-validation (LOOCV) R^2 statistics of the PLS-only model and the UK model (PLS +ordinary kriging) for each monitoring scenario, as well as the maximum likelihood estimates of the three empirical variogram

parameters. The best fitting variogram form used in the semivariogram plots is shown at the bottom of Table 2; the exponential variogram was used for NO_X and spherical variogram for O_3. The optimal number of PLS components based on the highest R^2 is also shown. For badge NO_X, one component was selected for both seasons, whereas for mobile NO_X, two components were selected for the summer and three for the winter. For mobile NO_X data, LOOCV R^2 increased by about 0.1–0.2 after UK, indicating that the model residuals had spatial correlation structure. For badge O_3 data, it was not possible to construct models, as no PLS component had any explanatory power; in both seasons, R^2 was very small. Models using mobile O_3 data were better, with R^2 from models with two PLS components of 0.71 and 0.58 in the summer and the winter, respectively. Kriging contributed substantially to model R^2 with the mobile data for NOx and O_3, but added little to the badge data models for NO_X.

Figures 3a and b is a graph of the 257 geographic variable loadings onto each of the two PLS component scores for NO_X and O_3 for mobile monitoring summer data. For NO_X, high positive loadings for the first component include population, number of major road intersections (A1 to A3), water land for large buffer sizes, nearby emission of pollutants, impervious surface, high- and medium-developed areas, and length of major road. High negative loadings include distance to features (coast, city hall, port), all NDVI scores, forest land use in larger buffers, and low-, open-development. Hence, the first score could be considered an “urbanization” component. The second PLS component is orthogonal to the first component, with high positive loadings from distance to some features (distance to A2 and A2–A2 or A3 intersections and airport), land use such as pasture, shrub, crop, and some near A3 roads, and major roads length and intersections. Barren land, and two kinds of wetland, and far emission of pollutants contribute to negative loadings. The second score could be considered as “traffic-related.”

For O_3, in contrast to NO_X, the positive loadings were largely of natural features for both components, whereas negative loadings were of features associated with development (urbanization). Also, distance to features (city hall, commercial area, distance to A3, and related intersections), near emissions, and length of far A1 roads have considerable positive loadings on the second component, in contrast to NO_X. For O_3, then, the first score generally reflects natural features, whereas the second score reflects more anthropogenic features.

For O_3, the PLS loadings on the two components were similar in the winter (data not shown). For NO_X, PLS loadings were also similar in the winter except for the addition of a third component with loadings reflecting largely water features (data not shown). Using badge NO_X, the one PLS component had similar feature loadings as the first mobile NOx component, for both seasons (data not shown), reflecting urbanization.

Model Performance and Predictions

Figure 4 shows predicted concentration (estimated from the UK models with the optimal number of components) plotted against observed concentration at the 43 monitoring sites, together with linear regression lines by season of predicted on observed with corresponding regression R^2. As noted above, no predictions could be made using the badge O_3 data. For NO_X, R^2 of predicted on observed concentrations were better using the mobile data than

the badge data, as were LOOCV R^2 (Table 2), particularly in the winter. For badge NO_X, based on either regression R^2 or LOOCV R^2, models performed equally well in the summer and the winter, but for mobile NO_X data, the winter model R^2 was better than the summer model. For the mobile O_3 data, the summer model performed somewhat better than the winter model. Agreement between observed and predicted was good for all models. The regression R^2 was generally slightly higher than the corresponding LOOCV R^2 from the UK model. Of note, although the model R^2 for the mobile NO_X data are uniformly good (Table 2 and Figure 4), based on the scatterplots (Figure 4), predictions from the model seem to over predict the observed data at low concentrations and underpredict at higher concentrations more than either the NO_X badge data model or the O_3 mobile data model.

Figures 5a–f show maps of predicted NO_X and O_3 concentrations at two levels of resolution and interpolated by ordinary kriging for display. Higher NO_X concentrations were in central Baltimore, and notably near the A1 and A2 roads in the less urban areas, especially with badge data. In contrast, O_3 higher concentrations were outside of central Baltimore and in a small area northwest of the city, whereas lower O_3 concentrations were found near A1 and A2 roads.

DISCUSSION

Summary

Exposure prediction models for O_3 and NO_X in Baltimore using a UK model with PLS-based LUR were developed from passive, time-integrated monitoring data and from mobile continuous monitoring data collected during peak traffic periods at the same monitoring sites and over the same time periods. Models based on the mobile modeling data performed well for both NO_X and O_3 in both the summer and winter seasons. The NO_X models based on the passive monitoring data also performed reasonably well, although not as well as those based on the mobile monitoring data. The passive O_3 monitoring data exhibited little spatial structure, which did not allow development of models using geographic variables and kriging.

The Monitoring Data

The purpose of comparing the utility of the two monitoring approaches was not to assess the comparability of the data generated by the two approaches, but rather to compare their respective utility in generating exposure prediction models. Clearly, average concentrations from the time-integrated passive badge data and the peak afternoon traffic data were not comparable. Average peak traffic O_3 concentrations from mobile monitoring in the summer were higher than the 2-week averaged values from badge samplers (Figure 2), reflecting the afternoon peak in summertime O_3 concentrations and the nighttime minima, despite the measurements being made on various sized roadways. NO_X concentrations did not show a similar pattern. NO_X concentrations from 1400 to 1700 hours were low, likely due to the increase in mixing depth and photochemical reactions, a pattern also seen at the AQS site. There was also some uncertainty in our NO_X measurements, with negative values being sometimes recorded, possibly obscuring differences if they were present. These negative

values were likely caused by O_3 and VOC interferences with the NO_X instrument we used, and may have obscured some of the spatial variability in NO_X.

A crucial and formidable problem in mobile monitoring is how to adjust for the influence of time on measurements made at different points in space. That is, pollution concentrations in an airshed change over time during the period of driving on any of the driving routes, so the contribution of temporal variation to the variability in spatial measurements should be removed to the extent possible. In essence, this entails estimating background concentrations. Brantley et al. recently reviewed several approaches for doing this, distinguishing approaches that use a site or sites considered to be representative of background, or using the time series of on-road measurement.[27] We elected to use our fixed site and the two AQS fixed sites for this purpose. Because of extensive missing data in our continuous fixed site monitoring data in the summer, we relied on AQS sites in the summer. One AQS site for NO_X was close to the one fuzzy point common to all three sampling loops, and for O_3, the AQS site located close to site 39 was used (Figure 1). Both sites were considered to reasonably represent the regional temporal variation in pollution concentrations. The use of afternoon averages of the fixed (AQS) site resulted in better model performance in the summer than the hourly data, based on LOOCV R^2 values. However, in the winter, corresponding hourly average values were preferred.

Model Performance

All of the PLS and UK models had good prediction accuracy based on the optimized LOOCV R^2 values (Table 2) for O_3 using the mobile monitoring data or, for NO_X, either the mobile or passive data. PLS for dimension reduction has been shown to be effective in this setting[25,28] and has advantages relative to other variable selection approaches. Second, the increase in LOOCV R^2 of the PLS-based UK models relative to the PLS-only models for the mobile monitoring data indicates that the residuals of the PLS regression models using the mobile monitoring data have more spatial structure than in models based on badge data, and this spatial structure could be used to further improve model performance. The performance of our NO_X model based on mobile monitoring data in the winter was generally better than or at least comparable to other efforts reported for NO, NO_2, and NO_X, with R^2 of 0.4–0.87.[1] Performance is also slightly better than our previously reported long-term NO_X spatio-temporal model using fixed monitoring site data (R^2 of 0.7–0.8),[29] and similar to those from Keller et al.[30] Our long-term O_3 exposure model performed similarly to others reported in the literature (R^2 = 0.4–0.6).[3,4]

Predictions from the NOx model based on mobile data overpredicted the observed data at low concentrations and underpredicted at higher concentrations, more than the predictions of the observed concentraitons from either the NOx badge data model or the O_3 mobile data model (Figure 4). One possible explanation for this behavior is that mobile monitoring was done on roadways, and fuzzy points were on roadways, albeit relatively less trafficked roadways. This would tend to enhance the contribution of roadway-related variables to the mobile NOx model. In the central urban area where NOx concentrations are higher, there are other sources of NOx other than traffic emissions which are unable to contribute much to the model, resulting in model underestimation of NOx concentrations. In contrast, outside

of the central urban area, traffic volume is less, although there are still many roadways. The roadway contribution to NOx in that setting is therefore less than what would be predicted, resulting in model overpredictions.

Badge O_3 Data Modeling

Badge O_3 monitoring data could not be used to build models for either the summer or winter seasons; either the geographic variables could not explain any of the spatial variation in O_3 concentrations or there was insufficient spatial variability in the badge O_3 concentrations. The badge data are cumulative and include concentrations over the full 24 h of each of the days included in the monitoring period. For a pollutant such as O_3, which has clear diurnal variation, the low nighttime values contribute substantially to the average. Nighttime concentrations in Baltimore were very low and even lower in rural sites resulting in homogenization of the cumulative average values measured by the badges. Findings from other studies using badge O_3 data have been similarly affected by this phenomenon.[31] The mobile monitoring data, on the other hand, were not affected in this way because they were only collected during periods when ambient O_3 concentrations were relatively high. Others have successfully built long-term O_3 exposure models using continuous fixed site measurements with diurnal temporal resolution.[3,4,32,33] Alternatively, O_3 spatial distributions could be different in other cities, which might allow badge data to be used. In light of our findings for NO_X, even when badge data can be used, they are likely inferior to other sources of monitoring data for the purpose of building highly resolved spatial models.

Limitations

Although our exposure prediction models performed well, there is room for improvement. First, the short monitoring campaigns in each of two seasons may not have been long enough to fully capture long-term spatial variability over an entire year. Also, each of the sites was only sampled using the mobile monitoring platform on 3 or 4 days of the monitoring period. Second, temporal adjustment plays a critical role in allowing the raw mobile monitoring data to be used in a spatial model. We used fixed sites for this purpose, but the sites and averaging times were not entirely consistent across season. Also, the sites used for time adjustment may not have adequately reflected the regional concentrations, depending on the pollutant and the season. It is possible that other approaches to time adjustment may work better. Third, meteorology, such as wind direction, was not taken into account in assessing spatial variability due largely to lack of meteorology monitoring at fine enough spatial resolution. This information, from finely resolved modeled meteorology, for example, may have allowed us to use the data to better capture spatial contrasts. Finally, because the reported findings were from a single city in a single year, generalization of the conclusions should be viewed cautiously.

CONCLUSIONS

Overall, our UK with PLS-based LUR exposure prediction models had good prediction accuracy. The NO_X models using mobile monitoring data performed better than models using passive badge data, whereas badge data could not be used at all for an O_3 model.

Although more resource intensive, mobile monitoring data are preferred over passively collected badge data for developing spatial exposure predictions, especially for O_3.

Supplementary Material

Refer to Web version on PubMed Central for supplementary material.

ACKNOWLEDGEMENTS

Wei Xu was supported by a scholarship awarded by the Chinese Scholarship Council. This publication was made possible by USEPA grant (RD-83479601-0). Its contents are solely the responsibility of the grantee and do not necessarily represent the official views of the USEPA. Further, USEPA does not endorse the purchase of any commercial products or services mentioned in the publication.

ABBREVIATIONS

AQS	Air Quality System
LOOCV	leave-one-out cross-validation
LUR	land use regression
PLS	partial least squares
UK	universal kriging

REFERENCES

1. Hoek G, Beelen R, de Hoogh K, Vienneau D, Gulliver J, Fischer P et al. A review of land-use regression models to assess spatial variation of outdoor air pollution. Atmos Environ 2008; 42: 7561–7578.
2. Briggs DJ, de Hoogh C, Guiliver J, Wills J, Elliott P, Kingham S et al. A regression-based method for mapping traffic-related air pollution: application and testing in four contrasting urban environments. Sci Total Environ 2000; 253: 151–167. [PubMed: 10843339]
3. Jerrett M, Burnett RT, Pope CA 3rd, Ito K, Thurston G, Krewski D et al. Long-term ozone exposure and mortality. New Engl J Med 2009; 360: 1085–1095. [PubMed: 19279340]
4. Adam-Poupart A, Brand A, Fournier M, Jerrett M, Smargiassi A. Spatiotemporal modeling of ozone levels in Quebec (Canada): a comparison of kriging, land-use regression (LUR), and combined Bayesian maximum entropy-LUR approaches. Environ Health Perspect 2014; 122: 970–976. [PubMed: 24879650]
5. Hart JE, Yanosky JD, Puett RC, Ryan L, Dockery DW, Smith TJ et al. Spatial modeling of PM10 and NO2 in the continental United States, 1985–2000. Environ Health Perspect 2009; 117: 1690–1696. [PubMed: 20049118]
6. Madsen C, Carlsen KCL, Hoek G, Oftedal B, Nafstad P, Meliefste K et al. Modeling the intra-urban variability of outdoor traffic pollution in Oslo, Norway - A GA(2) LEN project. Atmos Environ 2007; 41: 7500–7511.
7. Ross Z, English PB, Scalf R, Gunier R, Smorodinsky S, Wall S et al. Nitrogen dioxide prediction in Southern California using land use regression modeling: potential for environmental health analyses. J Expo Sci Env Epid 2006; 16: 106–114.
8. Gonzales M, Qualls C, Hudgens E, Neas L. Characterization of a spatial gradient of nitrogen dioxide across a United States-Mexico border city during winter. Sci Total Environ 2005; 337: 163–173. [PubMed: 15626387]
9. Brunekreef B Exposure science, the exposome, and public health. Environ Mol Mutagen 2013; 54: 596–598. [PubMed: 23444186]

10. Beelen R, Hoek G, Vienneau D, Eeftens M, Dimakopoulou K, Pedeli X et al. Development of NO2 and NOx land use regression models for estimating air pollution exposure in 36 study areas in Europe - The ESCAPE project. Atmos Environ 2013; 72: 10–23.
11. Kanaroglou PS, Jerrett M, Morrison J, Beckerman B, Arain MA, Gilbert NL et al. Establishing an air pollution monitoring network for intra-urban population exposure assessment: A location-allocation approach. Atmos Environ 2005; 39: 2399–2409.
12. Padro-Martinez LT, Patton AP, Trull JB, Zamore W, Brugge D, Durant JL. Mobile monitoring of particle number concentration and other traffic-related air pollutants in a near-highway neighborhood over the course of a year. Atmos Environ 2012; 61: 253–264.
13. Norris G, Larson T. Spatial and temporal measurements of NO2 in an urban area using continuous mobile monitoring and passive samplers. J Expos Sci Anal Environ Epidemiol 1999; 9: 586–593.
14. Larson T, Henderson SB, Brauer M. Mobile monitoring of particle light absorption coefficient in an urban area as a basis for land use regression. Environ Sci Technol 2009; 43: 4672–4678. [PubMed: 19673250]
15. Larson T, Garcia N, Covert D, Brauer M. Mobile monitoring of particulate black carbon concentrations in an urban area. Epidemiology 2006; 17: 479–479. [PubMed: 16810097]
16. Montagne D, Hoek G, Nieuwenhuijsen M, Lanki T, Pennanen A, Portella M et al. The association of LUR modeled PM2.5 elemental composition with personal exposure. Sci Total Environ 2014; 493: 298–306. [PubMed: 24950499]
17. Khoder MI. Diurnal, seasonal and weekdays–weekends variations of ground level ozone concentrations in an urban area in greater Cairo. Environ Monit Assess 2009; 149: 349–362. [PubMed: 18274871]
18. Reddy BSK, Kumar KR, Balakrishnaiah G, Gopal KR, Reddy RR, Ahammed YN et al. Observational studies on the variations in surface ozone concentration at Anantapur in southern India. Atmos Res 2010; 98: 125–139.
19. Riley EA, Banks L, Fintzi J, Gould TR, Hartin K, Schaal L et al. Multi-pollutant mobile platform measurements of air pollutants adjacent to a major roadway. Atmos Environ 2014; 98: 492–499.
20. National Geospatial Intelligence Agency. Ports of the Wider Caribbean, from NIMA World Port Index. Available: https://www.nga.mil/Pages/Default.aspx; 2013.
21. National Land Cover Database. NLCD 2006 Land Cover (2011 Edition). Available: http://www.mrlc.gov/nlcd2006.php; 2006.
22. Global Land Cover Facility. MODIS Normalized Difference Vegetation Index. Available: http://glcf.umd.edu/data/ndvi/; 2006.
23. U.S. Geological Survey. National Elevation Dataset. Available: http://nationalmap.gov/elevation.html; 2013.
24. U.S. EPA (U.S. Environmental Protection Agency). Emission Inventory Group. Available: http://www.epa.gov/air/emissions; 2006.
25. Sampson PD, Richards M, Szpiro AA, Bergen S, Sheppard L, Larson TV et al. A regionalized national universal kriging model using Partial Least Squares regression for estimating annual PM2.5 concentrations in epidemiology. Atmos Environ 2013; 75: 383–392.
26. Mevik B-HWR, Liland KH, pls: Partial Least Squares and Principal Component regression. R package version 23–0 2011.
27. Brantley HL, Hagler GSW, Kimbrough ES, Williams RW, Mukerjee S, Neas LM. Mobile air monitoring data-processing strategies and effects on spatial air pollution trends. Atmos Meas Tech 2014; 7: 2169–2183.
28. Bergen S, Sheppard L, Sampson PD, Kim SY, Richards M, Vedal S et al. A national prediction model for PM2.5 component exposures and measurement error-corrected health effect inference. Environ Health Perspect 2013; 121: 1017–1025. [PubMed: 23757600]
29. Mercer LD, Szpiro AA, Sheppard L, Lindstrom J, Adar SD, Allen RW et al. Comparing universal kriging and land-use regression for predicting concentrations of gaseous oxides of nitrogen (NOx) for the Multi-Ethnic Study of Atherosclerosis and Air Pollution (MESA Air). Atmos Environ 2011; 45: 4412–4420.
30. Keller JP, Olives C, Kim SY, Sheppard L, Sampson PD, Szpiro AA et al. A unified spatiotemporal modeling approach for predicting concentrations of multiple air pollutants in the Multi-Ethnic

Study of Atherosclerosis and Air Pollution. Environ Health Perspect 2014; 123: 301–309. [PubMed: 25398188]

31. Baxter LK, Dionisio KL, Burke J, Sarnat SE, Sarnat JA, Hodas N et al. Exposure prediction approaches used in air pollution epidemiology studies: key findings and future recommendations. J Expo Sci Env Epid 2013; 23: 654–659.
32. Liu LJS, Rossini AJ. Use of kriging models to predict 12-hour mean ozone concentrations in metropolitan Toronto - A pilot study. Environ Int 1996; 22: 677–692.
33. Araki SYK, Kondo A. Application of regression kriging to air pollutants concentrations in Japan with high spatial resolution. Aerosol Air Qual Res 2015; 15: 234–24.

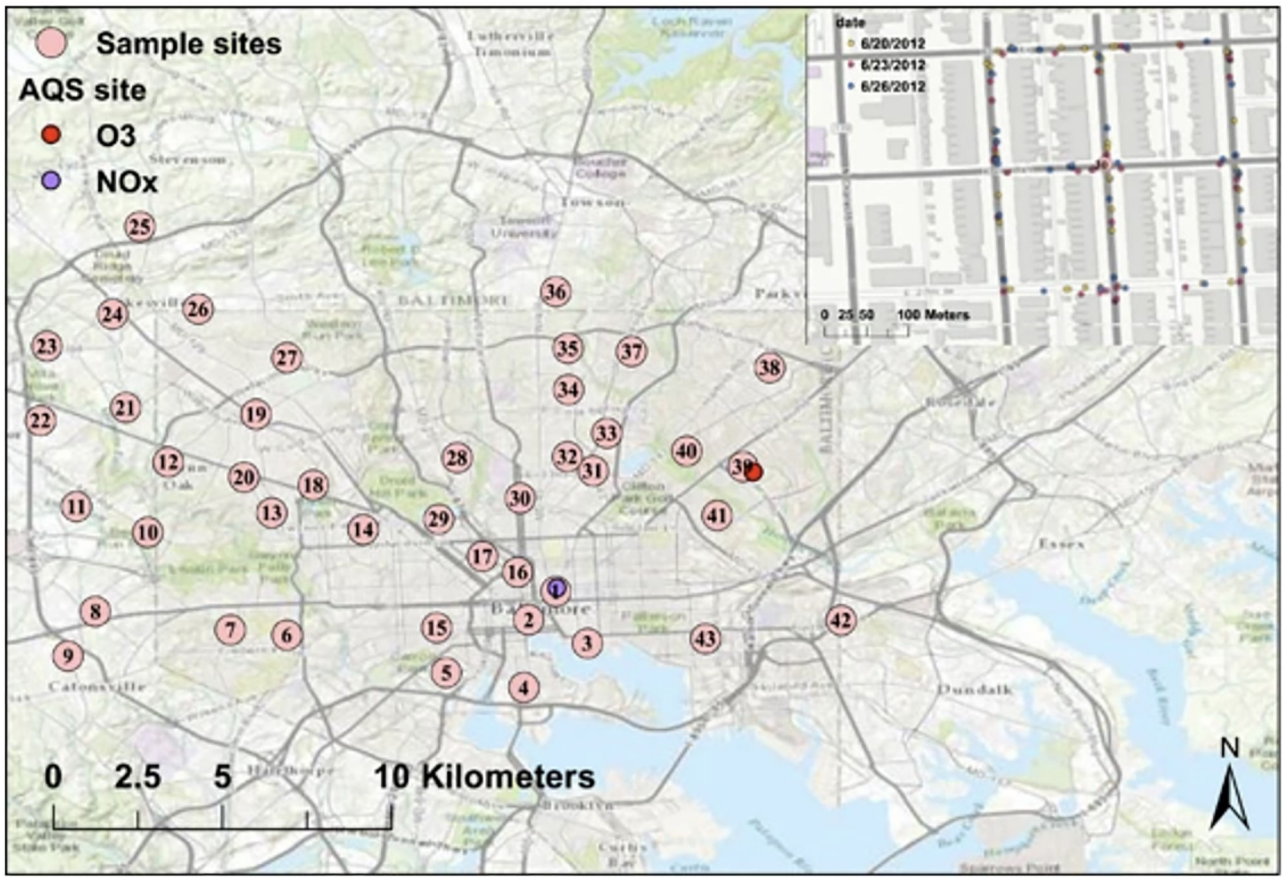

Figure 1.

Map of the central locations of 43 sample sites in Baltimore and 2 AQS monitor sites (red dot for O_3 and purple dot for NO_X). Inset map shows the mobile routes around site 30; dots are location of each 10 s measure.

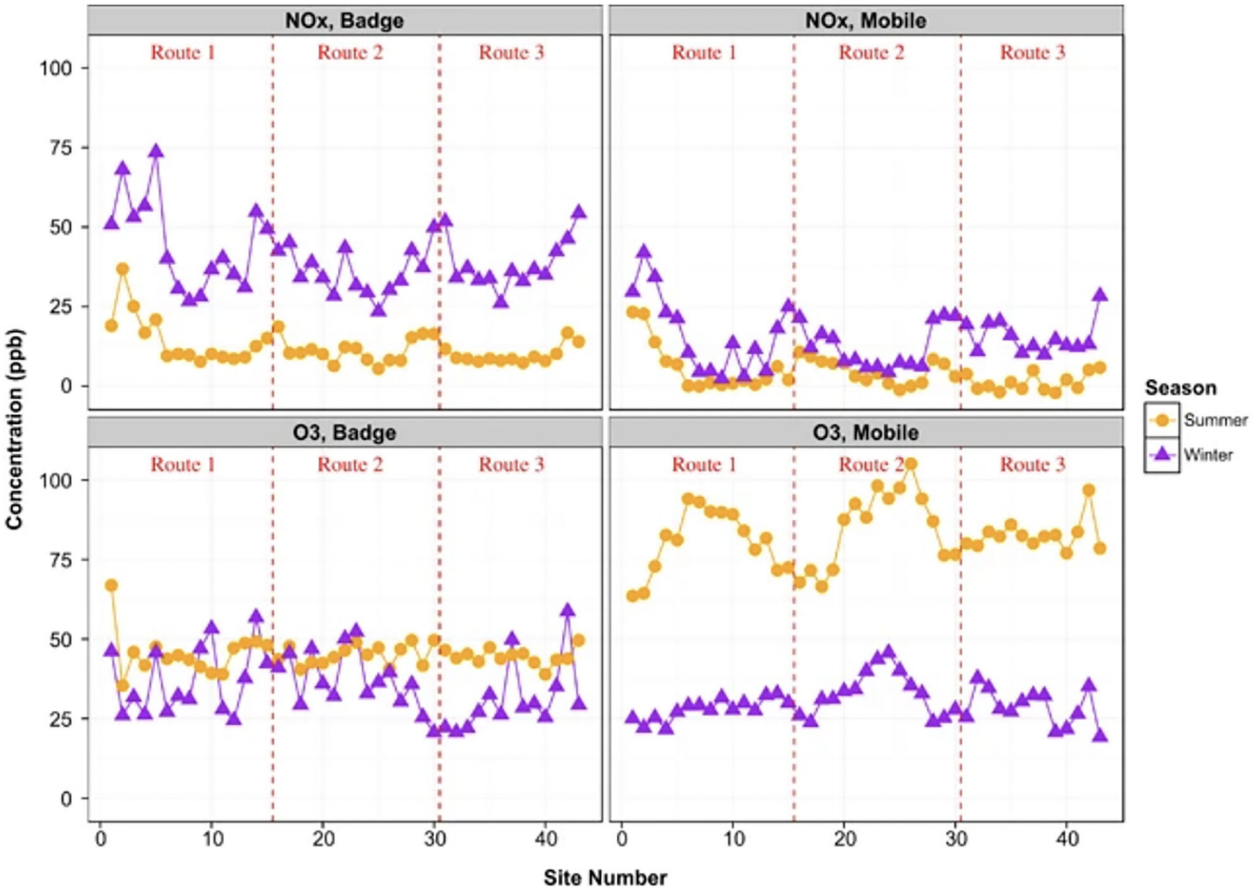

Figure 2.

Adjusted-median NO_X concentrations and adjusted-mean O_3 concentrations at 43 sites by monitoring approach and season. Two red dash lines in each panel divide sites into the three mobile monitoring routes. Each route was generally visited on the same day.

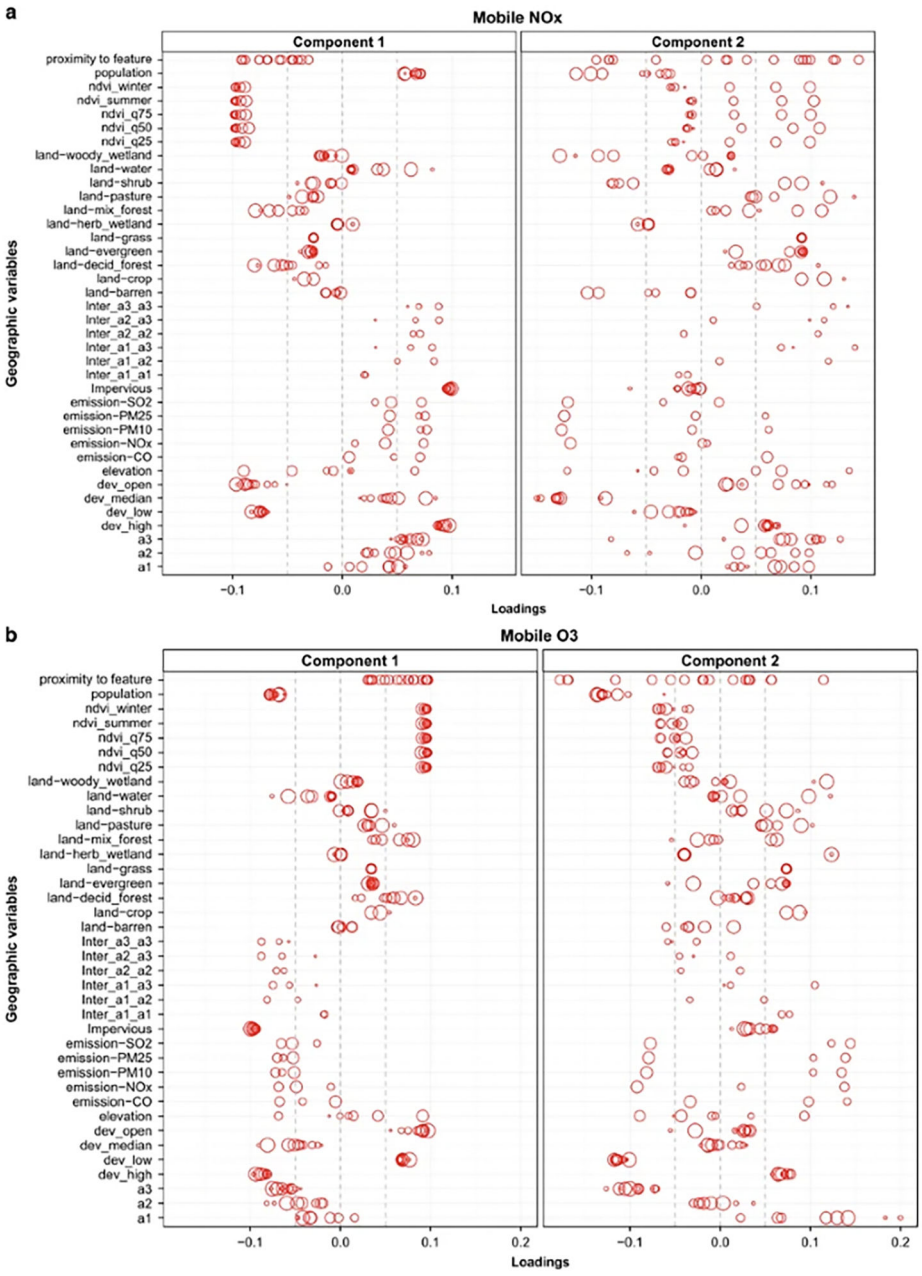

Figure 3.

(**a** and **b**) Loadings of the 257 geographic variables (Table 1) on the two PLS components for mobile NO_X and O_3 in the summer. The size of circles relates to buffer size, with increasing radius indicating larger buffer size.

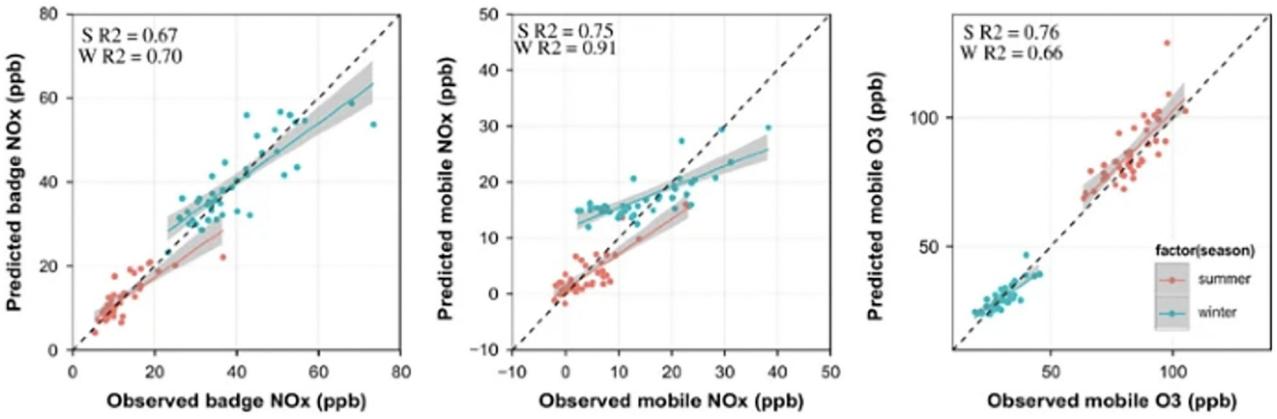

Figure 4.

Scatterplots of observed and predicted (from PLS + UK models) NO_X and O_3 data by season, with corresponding regression lines of predicted on observed and respective regression R^2. S and W indicates summer and winter, respectively.

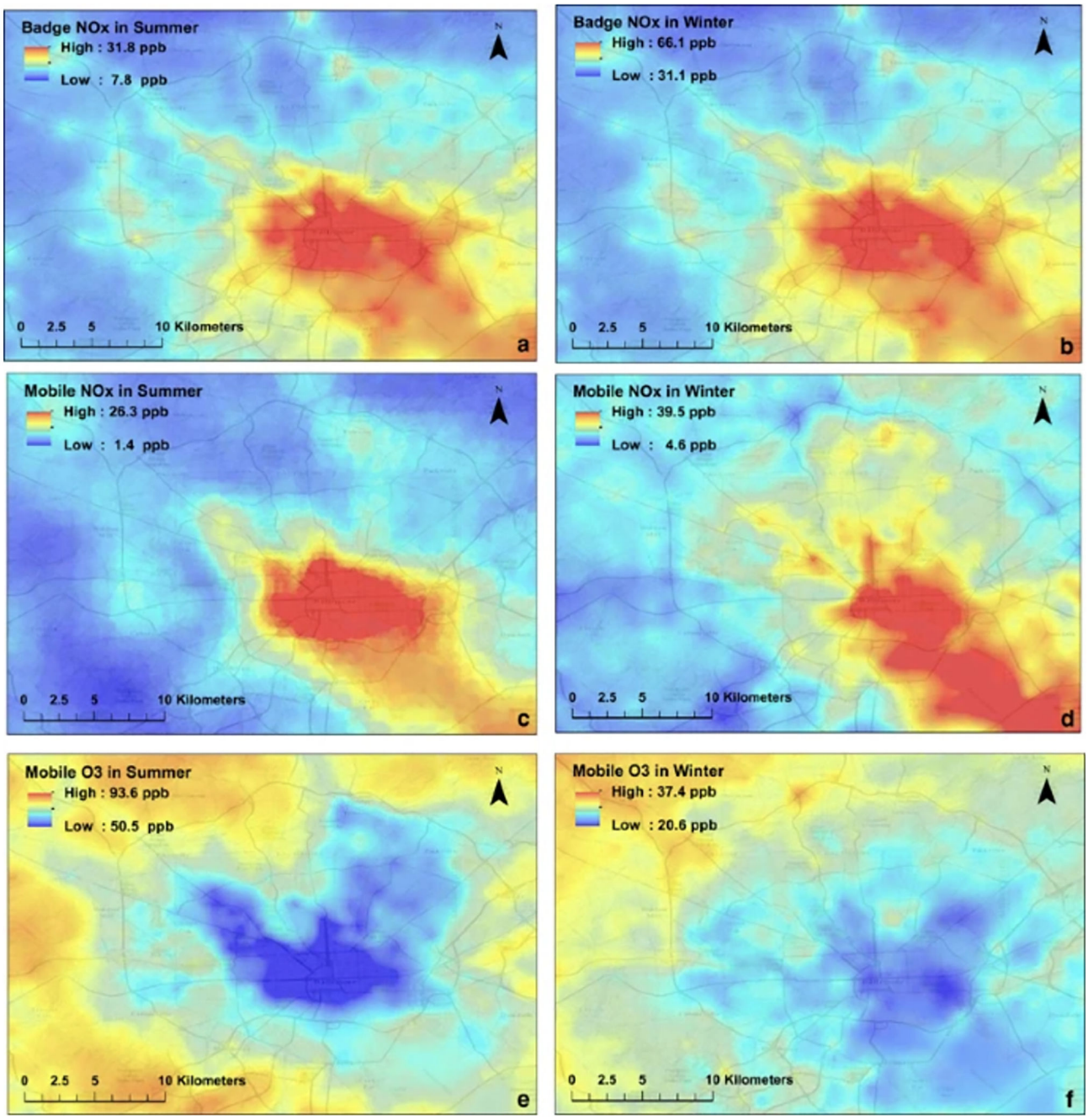

Figure 5.

Maps of predicted NO_x and O_3 concentration over the Baltimore area. (**a**) Badge NOx in summer; (**b**) badge NOx in winter; (**c**) mobile NOx in summer; (**d**) mobile NOx in winter; (**e**) mobile O3 in summer; mobile O3 in winter. The map is formatted with predicted concentrations at a 500-m grid resolution in central Baltimore and a 1-km grid resolution outside of central Baltimore. The raster images were computed in ArcGIS with ordinary kriging interpolation. Note that the color scales are different for each season.

Table 1

Geographic variables used in the PLS regression models.

Variable description	Details and buffer sizes (km)
Elevation	From sea level
Count of points of same elevation within or more than 20 or 50 m	Above, at, below 1 km and 5 km
Population (number)	0.5, 1, 1.5, 2, 2.5, 3, 5, 10, 15
Distance to nearest features: airport; large airport; large, medium, small port; railroad; rail yard; commercial zone; coastline; A1, A2, A3 roads	Not applicable
Emission: SO_2, NO_x, $PM_{2.5}$, PM_{10}, CO	3, 15, 30
Vegetative index (NDVI): 75th, 50th, 25th quartiles; winter; summer	0.25, 0.5, 1, 2.5, 5, 7.5, 10
Distance to main road intersection: A1–A1, A1–A2, A1–A3, A2–A2, A2–A3, A3–A3	0.5, 1, 3, 5
Lengths of main road: A1; A2; A3	0.05, 0.1, 0.15, 0.3, 0.4, 0.5, 0.75, 1, 1.5, 3, 5
Land use percentage: barren, crop, deciduous forest, mixed forest, evergreen, grass, herb, ice, pasture, shrub, water, woody wetland, high development, median development, low development, open development;	0.25, 0.5, 1, 2.5, 5, 7.5, 10
Average impervious surface (percentage)	0.05, 0.1, 0.15, 0.3, 0.4, 0.5, 0.75, 1, 3, 5

Table 2

Cross-validation R^2, kriging parameters (τ, σ, φ), and coefficients (β_0, β_1, β_2, β_3) of PLS+UK models for NOx and O_3 for the two monitoring approaches and seasons.

	NO_x Badge		**NO_x Mobile**		**O_3 Badge**		**O_3 Mobile**	
	Summer	**Winter**	**Summer**	**Winter**	**Summer**	**Winter**	**Summer**	**Winter**
# of PLS components	1	1	2	3	0	0	2	2
LOOCV R^2 of PLS	0.58	0.64	0.57	0.72	≈0.00	≈0.00	0.55	0.40
LOOCV R^2 of PLS+UK	0.60	0.65	0.70	0.90	–	–	0.71	0.58
Nugget (τ^2)[a]	0	0.295	0.137	0	–	–	0.0532	0.35
Partial sill (σ^2)[a]	0.33	0.0005	0.106	0.0895	–	–	0.0142	0.05
Range (φ^2, m)[a]	288.24	50.68	777.47	400.81	–	–	4326.57	2855.65
β_0	0.0025	0.000	−0.0058	0.004	–	–	9.08	5.43
β_1	0.818	0.083	0.0762	0.083	–	–	0.0395	0.036
β_2	–	–	–	0.140	–	–	0.0664	0.071
β_3	–	–	–	0.087	–	–	–	–
Variogram model[b]	Exp	Exp	Exp	Exp	–	–	Sph	Sph

[a] Kriging parameters are estimated from transformed data (Standardized for mobile NOx and square root transformed for all others).

[b] Exp, exponential function and Sph, spherical function, for the kriging models.